Performance of piezoelectric energy harvester with vortex-induced vibration and various bluff bodies

Adhes Gamayel[1], Mohamad Zaenudin[1], Brainvendra Widi Dionova[2]

[1]Department of Mechanical Engineering, Faculty of Engineering and Computer Science, Jakarta Global University, Depok, Indonesia
[2]Department of Electrical Engineering, Faculty of Engineering and Computer Science, Jakarta Global University, Depok, Indonesia

Article Info	ABSTRACT
	Piezoelectric energy harvesters (PEHs) are a kind of energy harvester that generates electricity due to pressure or vibration. Vortex-induced vibration (VIV) is a method that utilized wind energy and bluff body to generate the vibration in PEH. The objective of this research was to study the output voltage that generates in different bluff bodies with various airflow velocities. Experimental and simulation have done in this study. Experimental used PEH that consists of piezoelectric bimorph and rectangular-trapezoid fin. Bluff bodies with various cross-sectional areas, namely rhombus, square, and triangle were set up in front of the PEH at a distance of 80 cm. The various air velocities are set up to 5, 7, and 9 m/s in the wind tunnel with a cross-section of 250 mm × 250 mm. The simulation used the finite element method in explore the fluid flow pattern. The rhombus cross-sectional bluff body can generate voltage with an average of 1.5 volts. It is more voltage generated than a square and triangle. A vortex is formed near the rhombus bluff body and generates pressure fluctuation in its wake region. This pressure fluctuation takes place until airflow hits and leads PEH to vibrate and generate the voltage.

Corresponding Author:

Adhes Gamayel
Department of Mechanical Engineering, Faculty of Engineering and Computer Science
Jakarta Global University, Depok, Indonesia
Email: adhes@jgu.ac.id

1. INTRODUCTION

Nowadays, the critical problem in the world is the environmental pollutants and the energy crisis due to the increase of oil, coal, and other fossil fuels which will cause the depletion of fossil energy. These two critical issues trigger consideration of various clean, sustainable, and renewable energies such as solar energy, bioenergy, thermal energy, wind-energy, water-energy, and mechanical energy to replace fossil fuels [1]-[3]. Energy stands as one of the aspects that play a role in green economy-based development. Energy harvesting is a promising tool that can produce renewable energy and clean energy. This tool can increase the green economic utilization of infrastructure. Energy harvesting tools capture useless environmental ambient energy and convert it into more functional energy [4], [5]. Mechanical energy harvesting is a process that converts potential energy, kinetic energy, vibration energy, and deformation energy into electrical energy [6], [7]. Energy harvesting devices can collect and convert various forms of wasted energy into electrical energy for powering electronic circuits or devices. Vibration is one of the mechanical energies that is easy to produce. Vibration is the embodiment of mechanical energy in an elastic system of some sort continuously changing from mechanical kinetic to potential energy smoothly over and over again. Many conversions of mechanical energy (waste vibration) converted into electrical energy have been done using electromagnetic [8]-[10], piezoelectric [11]-[16], and electrostatic [17]-[20].

The piezoelectric energy harvesting system is related to the mechanical strength of energy harvesting using piezoelectric under large pressure and mechanical impedance matching, involving the electromechanical coupling factor of piezoelectric structure and piezoelectric comprising and coefficient electrical impedance [21]. Piezoelectric energy harvesters (PEH) have been widely used as a way to produce small electrical power for electronic devices due to their high energy density and easy integration system. A wind turbine combined with a piezoelectric energy harvester with flow-induced vortex-induced vibration was proposed to explore and to interpret the energy translation process. The piezoelectric is connected to the round bluff body and implemented at different wind speeds (2 m/s to 19 m/s). The maximum output that can be produced is about 8.97 μW at 19 m/s wind speed [22]. Design and built of the blub cylinder bluff body (circular and square cylinders) to maximize the output voltage and a quick increase with low wind speed range. The results indicate there is an increase in the average power generated by 75%. In addition, a slow wind speed will produce 193% greater output power than a reference using a square body bluff [23]. The bi-stable piezoelectric energy harvester (BPEH) was built to increase the efficiency of scavenging wind energy using a cruciform cantilever substrate (a circular cylinder, two square cylinders, a tip magnet, two external magnets, and PZT). The results show, for low wind speed vortex-induced vibration (VIV) takes effect and makes the system undergo snap-through while for high wind speed galloping happens and drives the system to execute snap-through. This BPEH can produce constant high-output energy in different speeds (low to high) [24].

However, the study of integrated design performance of energy harvesting systems is rare. The correlation of the bluff body with the piezoelectric energy harvesting needs to be observed. The main objective of this research is to study the fluid flow pattern through the bluff body and the effect of VIV in piezoelectricity to generate voltage. This research develops bimorph vortex-induced vibrations using a piezoelectric energy harvester on a wind tunnel with three different bluff body shapes (rhombus, square, and triangle) and various wind speeds (5 m/s, 7 m/s, and 9 m/s) based on the electrical energy produced and airflow pattern. The energy harvesting for wind tunnels using 3 types of bluff body shapes and 3 types of wind speed is analyzed and compared in this paper. Analysis of fluid flow pattern using the finite element method to explain the phenomena in the experimental result. Based on these results, the energy harvesting enhancement for the vortex-induced vibration energy harvester with the proposed bluff body and wind speed was obtained and discussed in this research.

2. METHOD

Generally, a typical PEH consists of a cantilever beam as a substrate layer in one (unimorph), two (bimorph), or multi-piezoceramic layers attached on its surfaces as the sensing or acting layers [25]. Unimorph is attached to a substrate where the one-layer piezoelectric material is laminated with different elastic stiffness. Two layers of laminated piezoelectric material on both sides of the substrate are called bimorphs. PEH called in this paper consist of piezoelectric bimorph and rectangular-trapezoid fin. Piezoelectric bimorphs used in this study are composed of lead zirconate titanate (PZT) and have the dimensions of 8 cm in height, 3 cm in width, and 0.6 mm in thickness. PZT is the most commonly used piezoelectric material due to its piezoelectric strain and stresses constantly being higher than other piezoelectric materials. PZT is a ferroelectric material in a polycrystalline form that has a maximum value of electromechanical coupling coefficients and dielectric. The properties of PZT that were used in this experiment are shown in Table 1.

A rectangular-trapezoid fin with material polypropylene has a length dimension of 12 cm and a width ratio dimension of 14:10 cm. It was added to the top of the piezoelectric with the purpose to expose the area where the wind blow causes the vibration. Bluff bodies with various cross-sectional areas, namely rhombus, square, and triangle were set up in front of the fin at 80 cm. Detail of PEH experimental setup and bluff body in the Figure 1 with Figure 1(a) configuration of head of wind tunnel, Figure 1(b) positional configuration of bluff body and PEH, and Figure 1(c) dimension of the bluff body used in the experiment.

Table 1. Material properties of PZT

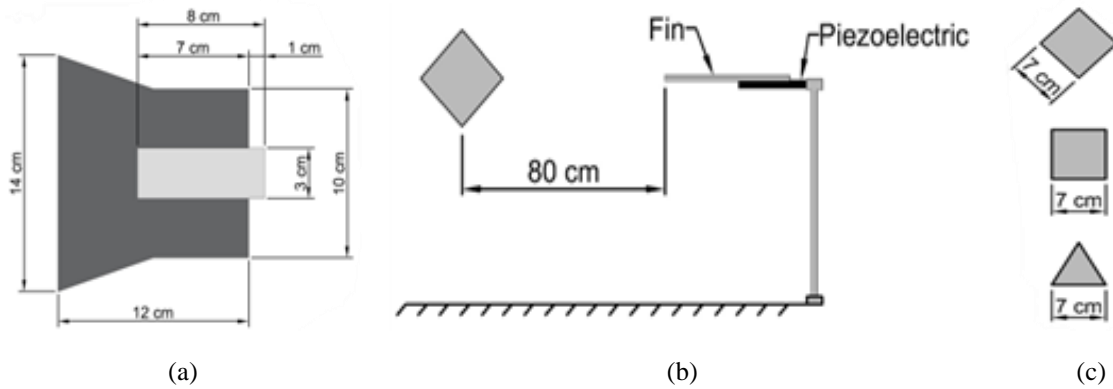| Properties	Unit	Value
Density	(10^3 kg/m^3)	7500
Young modulus	(GPa)	56
Poisson's ratio		0.36
Piezoelectric strain coefficient (d_{31})	Coulomb/Newton	-186×10^{-12}
Permittivity at constant stress ($\frac{\varepsilon_{11}}{\varepsilon_0}$)		3130
Permittivity at constant strain ($\frac{\varepsilon_{33}}{\varepsilon_0}$)		3400

Figure 1. Experimental setup with (a) PEH with head of wind tunnel; (b) bluff body and the position of PEH; and (c) dimension of the bluff body

Two experiments were implemented in this paper which are laboratory experimental and simulation methods. All of the units in the laboratory experiment were in the wind tunnel with a cross-section of 250 mm × 250 mm. A 12-inch blower with a power of 550 watts and static pressure of 350 Pa was generated by the wind blow in the tunnel. The various air velocities are set up in 5, 7, and 9 m/s and the anemometer used to measure it. To stabilize the incoming wind, mini tube pipes were equipped in the wind tunnel. This experiment was set up to investigate the performance of energy harvesting in Figure 2. Data acquisition using DATAQ DI-245 with the setup duration of the measurement in 60 seconds with a record of 25 data per second. The objective of this experimental research was to study the output voltage that generates in different bluff bodies with various airflow velocities.
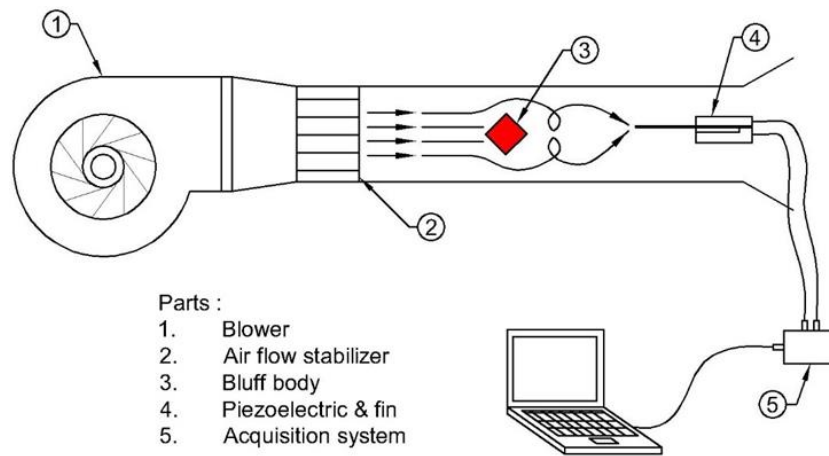

Figure 2. Experimental set-up

The simulation method used computational fluid dynamics with the software Fluent Solver Ansys R2 2020. The scope of work in this study includes creating geometry based on experimental material, meshing, determining the boundary type, deciding the solver, and analyzing the outcomes. AutoCAD Autodesk was used to draw the geometry and saved in format SAT file (*.sat) for suitable use in Ansys Workbench for educational purposes. Meshing is a step to perform accurate simulation by arranging elements containing nodes to represent geometric shapes. The number of elements was set up for rhombus, triangle, and square namely in 474030, 458583, 488227, and nodes of 90716, 87941, and 93086. The boundary condition was set close to the experimental, in which the inlet area consists of air velocities 5, 7, and 9 m/s and the turbulence intensity of 5% under boundary circumstances. The air properties are set to absolute viscosity $1.859 \times 10\text{-}5$ N.s/m^2, density 1.17 kg/m^3 with operational at room temperature 27 °C. K-epsilon $(k - \varepsilon)$ was used as a turbulence model in this simulation. This model consists of two transport equations of turbulence which are turbulent energy (k) and dissipation of turbulent kinetic energy (ε). A three-dimensional (3-D) flow simulation technique with a high level of precision is used to get accurate and reliable results computationally.

The air from the blower is flowing through the stabilizer and set to meet the rhombus bluff body, thus allowing the airflow to create a turbulent effect which then deforms the piezoelectric fin and generates elastic waves. This method is deployed based on a cantilever, where the piezoelectric fin will move around and produce a longitudinal and transversal displacement thus allowing the generation of electricity. Displacement of the piezoelectric fin is one of the key aspects to generating electricity, thus the analysis of this displacement is necessary for understanding the generation of electricity with piezoelectric. In this case, the displacement field at time t and beam point x has components,

$$[u, w]^\top = \left[-z\frac{\partial w}{\partial x}, w\right]^\top \tag{1}$$

Where $u(x, t)$ represents the longitudinal displacement and $w(x, t)$ represents the transversal displacement in the mid-plane where the elastic deformation most likely occurs.

The simulation aimed to explore the airflow pattern between the bluff body and PEH in the wind tunnel. The result of the simulation shows the area with minimum and maximum air velocity in the wind tunnel. This Ansys result is used to analyze the correlation of generated voltage with the vibration possibility due to the flow pattern through the bluff body.

3.   RESULTS AND DISCUSSION
3.1. Experimental result

The result of output voltage in energy harvesting experiments using piezoelectric and bluff bodies is shown in Figure 3 with different air velocity, they are Figure 3(a) 5 m/s, Figure 3(b) 7 m/s, and Figure 3(c) 9 m/s. Based on Figure 3, the graph of the output voltage fluctuations due to the unstable vortex taking the air to hit the PEH. The unstable vortex affects the lift force and drag force in PEH and has bad synchronization in oscillation. Cantilever systems that are used to stand the piezoelectric create the motion of PEH upward and downward when the air velocity hits them. This up-and-down movement generates the output voltage in negative and positive results that describe the voltage as an alternate current (AC). The experimental result was found that a bluff body with a rhombus cross-sectional area can generate voltage more than a triangle and square. It is due to the shape of the rhombus bluff body that might have produced more vortex than triangle and square. When fluid flows around a bluff body, the vortex occurs periodically in the wake behind the bluff body [2]. Besides that, the inlet area in the wind tunnel becomes narrow due to the presence of a bluff body, and leads to an increase in air velocity. With a similar length of the side, the presence of a rhombus cross-sectional bluff body leads the inlet area narrower than the triangle and square.

A comparison of the bluff body in generating peak and average voltage with increased air velocity is shown in Figure 4. Rhombus is the greatest cross-sectional bluff body in this experiment to generate peak voltage in 5, 7, and 9 m/s namely 3.98-volt, 5.15-volt, and 5.58-volt. Triangle bluff bodies have less output voltage, namely 1.95-volt, 2.6-volt, and 3.59-volt. Rhombus gets a maximum average voltage of 1.53 volts higher than square and triangle. Gap voltage found in peak and average voltage. Peak voltage occurs once and average voltage means that the amplitude has a range of 0 to 1.5 volts. The conversion of mechanical power to electrical power is obtained from the great performance of the amplitude [26]. The amplitude addressed to good oscillation in the sinusoidal wave. To generate more voltage, the amplitude must increase in number where the factor to improve the performance of PEH such as stiffness and piezoelectric effect correlate it. Stiffness identifies the material as difficult to deflect or having minimum deflection when the load takes place on the material. The piezoelectric effect takes place when mechanical pressure or load change the polarization of electrons in a material. More stiffness in PEH causes the piezoelectric effect to be minimum and the amplitude to be small. Therefore, the oscillations and output voltages generated are minimal. The output voltage in Figure 4 increased along with the increase of the air velocity for all of the bluff bodies. The air velocity through the bluff body has a greater influence on the output voltage energy. When the blower generates circular airflow through the bluff body, it is induced to vibrate as a series of regular and irregular vortex shedding. The rise of air velocity led to an increase in the force that created more deformation in the PEH. It is caused mainly by the influence of the turbulence which induces the vortex street instability, and then leads to fluctuating oscillation of output voltage. Impulse and momentum take place during the vortex street instability, where the initial force from the air velocity hits the PEH. The deformation of the piezoelectric film with the stress is directly connected to the output electric voltage based on the piezoelectric effect [22].
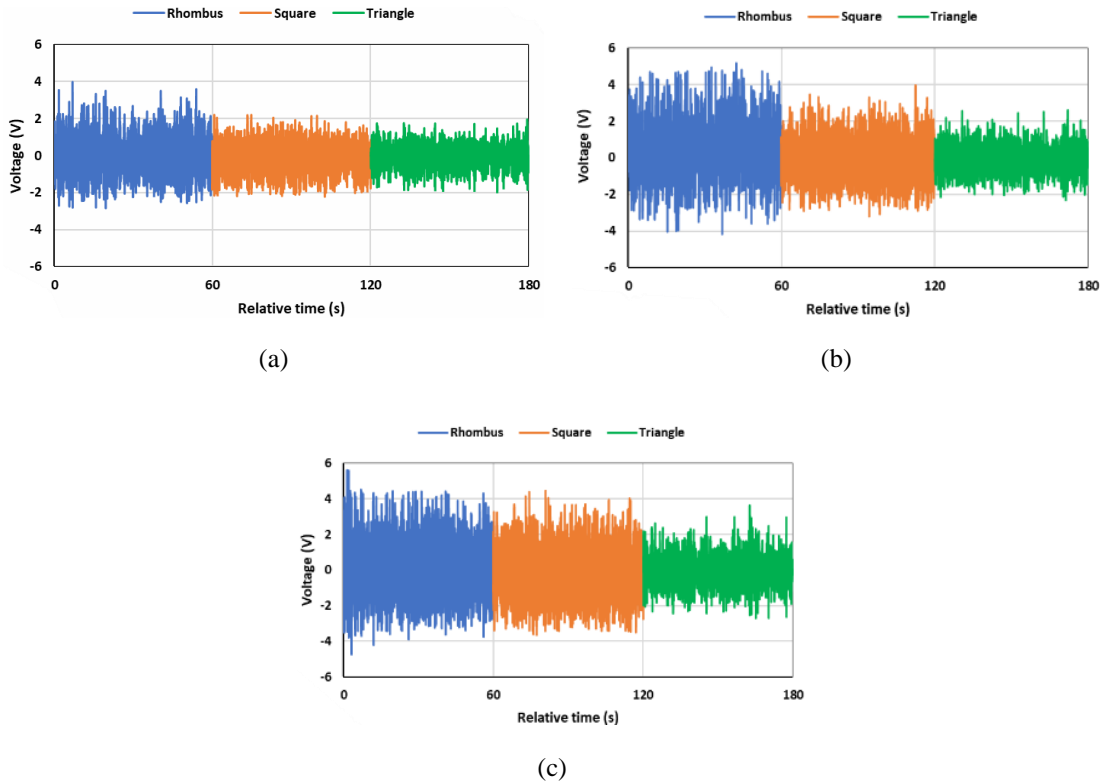
(a)

(b)

(c)

Figure 3. Voltage produced with various air velocity: (a) 5 m/s, (b) 7 m/s, and (c) 9 m/s
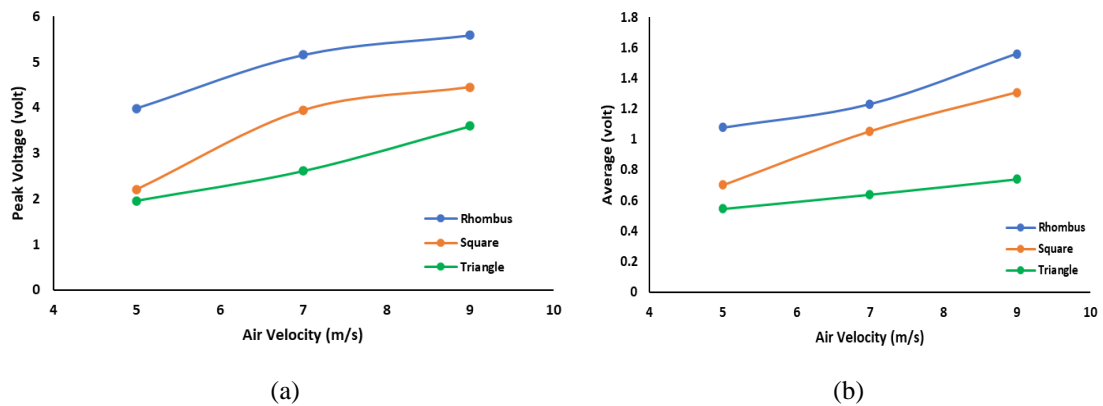

(a)

(b)

Figure 4. Voltage produced by different air velocity and bluff bodies: (a) peak voltage and (b) average voltage

3.2. Simulation result

Figure 5 shows the flow separation and vortex evolution when the airflow is through the bluff body. The different air velocity inlet in every bluff body has different maximum air velocity. The rhombus bluff body has increased the air velocity at maximum, namely 11.33 m/s, 15.69 m/s, and 22.6 m/s. Triangle bluff bodies have raised the air velocity to a maximum fewer than rhombus, namely 9.7 m/s, 13.64 m/s, and 17.57 m/s. Rhombus and square bluff bodies have similar airflow patterns and velocities. It's due to the symmetrical shapes leading the flow pattern similar in upside and downside wind tunnel. The different airflow patterns take place in the triangle bluff body due to the placement position in the base of a lower position leading to airflow patterns in the upside and downside drawn unsymmetrical. The different airflow pattern leads to the airflow velocity that hits the PEH for the triangle higher than the rhombus and the square bluff body. Generally, the best maximum airflow velocity and the largest area of velocity vector are generated with the rhombus due to the position of the rhombus at the inlet area in the wind tunnel becoming narrow and leading to the air velocity increase.
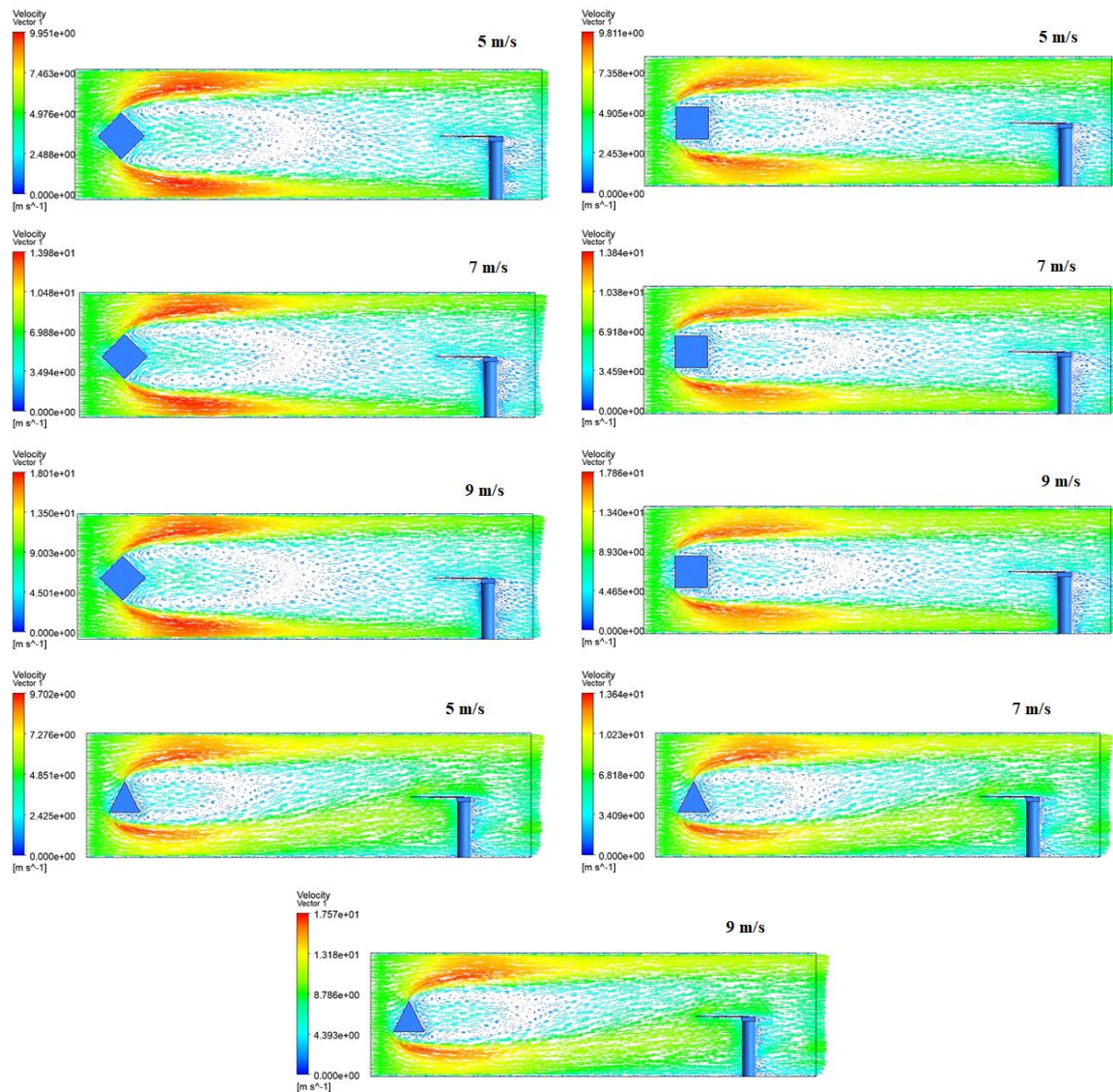
Figure 5. Simulation result in velocity vector

When the airflow passes through the bluff body, the air velocity increases along the walls of the wind tunnel. Increasing the airflow velocity in all bluff bodies attributes to the wake disturbance becoming stronger. The deformation of PEH increases when wake intensity increases. Besides that, a vortex is formed near the bluff body and generates pressure fluctuation in its wake region. This pressure fluctuation takes place until PEH vibrates. Airflow was separated after through the rhombus and square bluff body. It raised a fluctuating force perpendicular to the direction of the flow. Many vortices are created when the airflow through to this bluff body. Triangular bluff bodies have vortices in the wake region, but less in the PEH area leading to the minimum fluctuation in PEH. Based on the Bernoulli equation, the minimum velocity has maximum pressure. It indicates that the higher-pressure fluctuation in both bluffs occurs evenly in surface PEH. Higher pressure causes the deflection of PEH to be upward and downward. It makes the PEH vibrate and then generates a voltage in relatively high numbers. When the hit area occurs in a vortex shed, the force can generate the PEH to move upward and downward simultaneously. Triangle bluff bodies generate higher airflow velocity than others when the airflow hits the PEH with minimum vortices shed. This event leads the PEH to move upward and get the minimum frequency to down due to minimum pressure fluctuation and vortex shedding in that area. Thus, the output voltage in Figure 3 has a correlation with the velocity vector in Figure 5, where the output voltage generated by the triangle bluff body is the lowest due to the highest velocity vector in the strike line mode hitting the PEH and making the PEH leaning upward with minimum deflection.

Figure 6 shows the pressure vector in airflow through the different bluff bodies. The periodic vortex shedding generates asymmetric pressure distribution that provides the periodic force which consequently leads to vibration. The high-pressure attribute more often the periodic vortex shedding takes place in the wake region. The pressure vector has a positive and negative number. A positive number means the surface of the bluff body is directly in contact or hit by air. A negative number means low pressure as a result of the separation of airflow in the wake region. The result of pressure shows a negative number for the wake region in the square and triangle bluff body. But the rhombus bluff body shows a positive number. The wake region in the rhombus bluff body has higher pressure than squares and triangles. It's led PEH to vibrate more often and generate more output voltage.
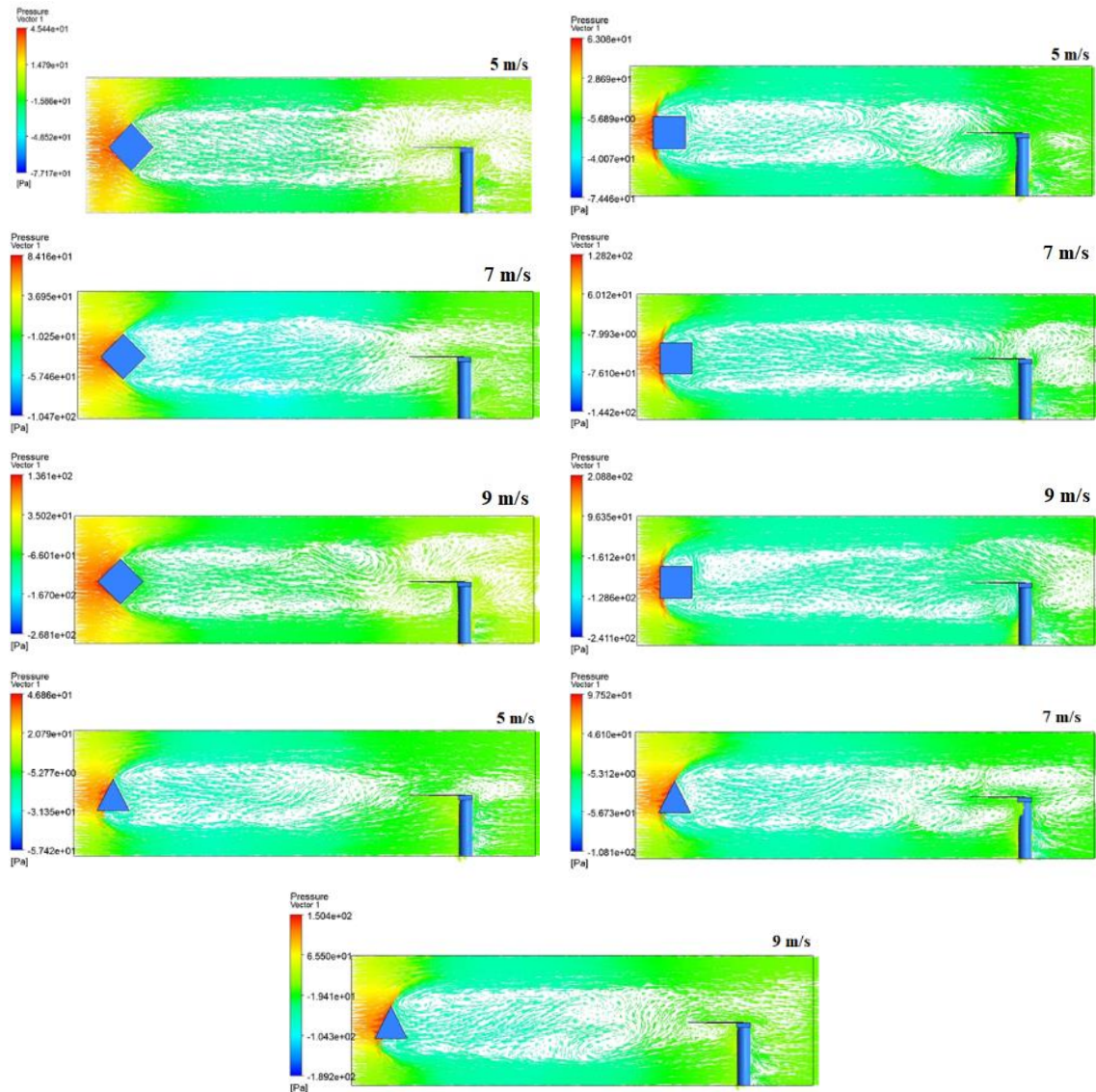
Figure 6. Pressure vector in various bluff body

4. CONCLUSION

PEH with the different bluff bodies with various airflow velocities has been tested in the wind tunnel and simulated using Ansys Academic version. The highest peak voltage in this experiment is 5.58 volts with a voltage average of 1.53 volts. It was found that a bluff body with a rhombus cross-sectional area can generate more voltage than a triangle and square. The simulation result confirms that airflow passing through the rhombus bluff body has maximum velocity and leads to a minimum pressure in the wind tunnel wall. It generates pressure fluctuation in its wake region until airflow hits and leads PEH to vibrate and generate the voltage.

REFERENCES

[1]   H. Liu, J. Zhong, C. Lee, S. -W. Lee, and L. Lin, "A comprehensive review on piezoelectric energy harvesting technology: Materials, mechanisms, and applications," *Applied Physics Reviews*, vol. 5, no. 4, 2018, doi: 10.1063/1.5074184.
[2]   J. Wang, L. Geng, L. Ding, H. Zhu, and D. Yurchenko, "The state-of-the-art review on energy harvesting from flow-induced vibrations," *Applied Energy*, vol. 267, 2020, doi: 10.1016/j.apenergy.2020.114902.
[3]   F. Qian, T. -B. Xu, and L. Zuo, "Piezoelectric energy harvesting from human walking using a two-stage amplification mechanism," *Energy*, vol. 189, 2019, doi: 10.1016/j.energy.2019.116140.
[4]   H. Wang, A. Jasim, and X. Chen, "Energy harvesting technologies in roadway and bridge for different applications – A comprehensive review," *Applied Energy*, vol. 212, pp. 1083–1094, 2018, doi: 10.1016/j.apenergy.2017.12.125.
[5]   K. Y. Fang, W. Q. Jing, Y. F. He, Y. C. Zhao, and F. Fang, "A low-frequency vibration energy harvester employing self-biased magnetoelectric composite," *Sensors and Actuators A: Physical*, vol. 332, 2021, doi: 10.1016/j.sna.2021.113066.
[6]   S. Zargari, Z. D. Koozehkanani, H. Veladi, J. Sobhi, and A. Rezania, "A new Mylar-based triboelectric energy harvester with an innovative design for mechanical energy harvesting applications," *Energy Conversion and Management*, vol. 244, 2021, doi: 10.1016/j.enconman.2021.114489.
[7]   Z. Yang, S. Zhou, J. Zu, and D. Inman, "High-Performance Piezoelectric Energy Harvesters and Their Applications," *Joule*, vol. 2, no. 4, pp. 642–697, 2018, doi: 10.1016/j.joule.2018.03.011.
[8]   S. -C. Kim, J. -G. Kim, Y. -C. Kim, S. -J. Yang, and H. Lee, "A Study of Electromagnetic Vibration Energy Harvesters: Design Optimization and Experimental Validation," *International Journal of Precision Engineering and Manufacturing-Green Technology*, vol. 6, pp. 779–788, 2019, doi: 10.1007/s40684-019-00130-4.
[9]   Y. Li, C. Zhou, Q. Cao, X. Wang, D. Qiao, and K. Tao, "Electromagnetic vibration energy harvester with tunable resonance frequency based on stress modulation of flexible springs," *Micromachines*, vol. 12, no. 9, 2021, doi: 10.3390/mi12091130.
[10]   H. Azam, N. H. H. M. Hanif, and A. A. M. Ralib, "Magnetically plucked piezoelectric energy harvester via hybrid kinetic motion," *IIUM Engineering Journal*, vol. 20, no. 1, pp. 245–257, 2019. [Online]. Available: http://irep.iium.edu.my/79712/1/79712-Magnetically%20plucked%20piezoelectric.pdf
[11]   S. Ju and C. -H. Ji, "Impact-based piezoelectric vibration energy harvester," *Applied Energy*, vol. 214, pp. 139–151, 2018, doi: 10.1016/j.apenergy.2018.01.076.
[12]   Y. Cao and H. Huang, "Design and optimization of variable stiffness piezoelectric energy harvesters," *Composite Structures*, vol. 285, 2022, doi: 10.1016/j.compstruct.2022.115204.
[13]   C. Dagdeviren *et al.*, "Recent progress in flexible and stretchable piezoelectric devices for mechanical energy harvesting, sensing and actuation," *Extreme Mechanics Letters*, vol. 9, pp. 269–281, 2016, doi: 10.1016/j.eml.2016.05.015.
[14]   N. H. H. M. Hanif, M. Z. Zain, M. E. Rohaimie, and H. Azam, "Power estimation for wearable piezoelectric energy harvester," *TELKOMNIKA (Telecommunication Computing Electronics and Control)*, vol. 16, no. 3, pp. 983–988, 2018, doi: 10.12928/TELKOMNIKA.v16i3.9034.
[15]   A. A. M. Ralib, N. W. A. Zulfakher, R. A. Rahim, N. F. Za'Bah, and N. H. H. M. Hanif, "Finite element simulation of mems piezoelectric energy scavenger based on PZT thin film," *IIUM Engineering Journal*, vol. 20, no. 1, pp. 90–99, 2019, doi: 10.31436/iiumej.v20i1.991.
[16]   M. S. M. Tahir, N. H. H. M. Hanif, and A. N. Wahid, "Maximizing Output Voltage of a Piezoelectric Energy Harvester Via Beam Deflection Method for Low-Frequency Inputs," *IIUM Engineering Journal*, vol. 23, no. 1, pp. 434–446, 2022, doi: 10.31436/IIUMEJ.V23I1.2156.
[17]   B. Vysotskyi, F. Parrain, X. L. Roux, E. Lefeuvre, P. Gaucher, and D. Aubry, "Electrostatic vibration energy harvester using multimodal-shaped springs for pacemaker application," in *2018 Symposium on Design, Test, Integration & Packaging of MEMS and MOEMS (DTIP)*, 2018, pp. 1-6, doi: 10.1109/DTIP.2018.8394216.
[18]   Y. Naito and K. Uenishi, "Electrostatic MEMS vibration energy harvesters inside of tire treads," *Sensors*, vol. 19, no. 4, 2019, doi: 10.3390/s19040890.
[19]   Y. Zhang, T. Wang, A. Luo, Y. Hu, X. Li, and F. Wang, "Micro electrostatic energy harvester with both broad bandwidth and high normalized power density," *Applied Energy*, vol. 212, pp. 362–371, 2018, doi: 10.1016/j.apenergy.2017.12.053.
[20]   B. D. Truong, C. P. Le, and E. Halvorsen, "Analysis of MEMS electrostatic energy harvesters electrically configured as voltage multipliers," *AEU - International Journal of Electronics and Communications*, vol. 107, pp. 125–136, 2019, doi: 10.1016/j.aeue.2019.05.006.
[21]   C. Covaci and A. Gontean, "Piezoelectric energy harvesting solutions: A review," *Sensors*, vol. 20, no. 12, 2020, doi: 10.3390/s20123512.
[22]   X. Du, M. Zhang, H. Chang, Y. Wang, and H. Yu, "Micro windmill piezoelectric energy harvester based on vortex-induced vibration in tunnel," *Energy*, vol. 238, 2022, doi: 10.1016/j.energy.2021.121734.
[23]   W. Sun, S. Jo, and J. Seok, "Development of the optimal bluff body for wind energy harvesting using the synergetic effect of coupled vortex induced vibration and galloping phenomena," *International Journal of Mechanical Sciences*, vol. 156, pp. 435–445, 2019, doi: 10.1016/j.ijmecsci.2019.04.019.
[24]   W. Qin, W. Deng, J. Pan, Z. Zhou, W. Du, and P. Zhu, "Harvesting wind energy with bi-stable snap-through excited by vortex-induced vibration and galloping," *Energy*, vol. 189, 2019, doi: 10.1016/j.energy.2019.116237.
[25]   P. Hajheidari, I. Stiharu, and R. Bhat, "Analysis of bimorph piezoelectric beam energy harvesters using superconvergent element," *Journal of Intelligent Material Systems and Structures*, vol. 30, no. 15, 2019, doi: 10.1177/1045389X19862360.
[26]   J. Lian, X. Yan, F. Liu, and J. Zhang, "Analysis on Flow Induced Motion of Cylinders with Different Cross Sections and the Potential Capacity of Energy Transference from the Flow," *Shock and Vibration*, 2017, doi: 10.1155/2017/4356367.

BIOGRAPHIES OF AUTHORS

Adhes Gamayel ⬤ 🆂 🆂🅲 ⬡ received the B.Eng. degree and the master's degree in mechanical engineering from the University of Brawijaya, Malang, Indonesia, in 2000 and 2007, respectively. The Ph.D. degree in mechanical engineering from the Management and Science University, Shah Alam, Malaysia, in 2021. He is currently a senior lecturer in Jakarta Global University. He has published 3 (three) books where two are tutorial in finite element method. He also has two intellectual properties right in industrial design. His current research interests in renewable energy, biofuel, mechanical design and analytical in finite element method. He can be contacted at email: adhes@jgu.ac.id.

Mohamad Zaenudin ⬤ 🆂 🆂🅲 ⬡ currently working as lecturer at Jakarta Global University, Depok and heading the Department of Mechanical Engineering. His research interest is in the field of materials science related to metallic material, especially dealing with molecular dynamics simulation. He has published several research papers in various journal ranging from international conference to international journal indexed on Scopus and ISI. Mr. Zaenudin received his bachelor from Universitas Negeri Jakarta and master from Management & Science University. He wins several research and academic grants. He can be contacted at email: mzaenudin@jgu.ac.id.

Brainvendra Widi Dionova ⬤ 🆂 🆂🅲 ⬡ is a lecturer in Electrical Engineering Department from Jakarta Global University, Jakarta, Indonesia. He is currently the Head of Department Industrial Engineering in Jakarta Global University (JGU). He received his S.ST (Bachelor) degrees in Industrial Electrical Engineering Electronic Engineering Polytechnic Institute of Surabaya (EEPIS) and M.Sc. Eng (Master) degrees in Electrical Engineering Management and Science University (MSU). His research interests include renewable energy (Photovoltaic and wind turbine), power electronic, motor drives, intelligent control and energy management. He can be contacted at email: brainvendra@jgu.ac.id.